

Benchmark potential energy curve for collinear H₃

Dávid Ferenc^a, Edit Mátyus^{a,*}

^aELTE, Eötvös Loránd University, Institute of Chemistry, Pázmány Péter sétány 1/A, Budapest, H-1117, Hungary

Abstract

A benchmark-quality potential energy curve is reported for the H₃ system in collinear nuclear configurations. The electronic Schrödinger equation is solved using explicitly correlated Gaussian (ECG) basis functions using an optimized fragment initialization technique that significantly reduces the computational cost. As a result, the computed energies improve upon recent orbital-based and ECG computations. Starting from a well-converged basis set, a potential energy curve with an estimated sub-parts-per-billion precision is generated for a series of nuclear configurations using an efficient ECG rescaling approach.

Keywords: H₃, ECG

PACS: 0000, 1111

2000 MSC: 0000, 1111

1. Introduction

The simplest chemical reaction H₂ + H → H + H₂—and its isotopologues—is possibly one of the most exhaustively studied chemical processes [1]. Furthermore, the H₃ system has qualitatively interesting features: a shallow van-der-Waals minimum for collinear nuclear structures and a conical intersection for equilateral triangular configurations. These features impose challenges when investigating the quantum dynamics of the system and require a high-level description of the electronic structure. The first potential energy surface (PES) for collinear H₃ was obtained by Liu in 1973 [2]. Since then, several full-dimensional surfaces have been published [3, 4, 5, 6, 7, 8, 9] and refined [10, 11, 12, 13, 14, 15, 16] using increasingly accurate quantum chemical methods. More recently, a multireference configuration interaction (MRCI) PES was developed, using a hierarchy of correlation consistent basis sets followed by extrapolation to the complete basis set (CBS) limit [17] with an estimated μE_h level of precision. This complete configuration interaction (CCI) surface has been the most accurate full-dimensional PES of H₃, and it was used to resolve long-standing discrepancy of experimental and theoretical thermal rate constants [18].

The first computation for this system using explicitly correlated Gaussian (ECG) basis functions

was performed by Cafiero and Adamowicz [19]. They determined the stationary points of the PES by the simultaneous minimization of the energy with respect to both the nonlinear parameters of the basis functions and the nuclear configuration using analytic gradients. Nevertheless, using only 64 basis functions, they obtained an energy, $-1.673\,467\,E_h$, which is above the dissociation threshold, $E(H_2) + E(H) = -1.674\,475\,714\,E_h$.

In later work, Pavanello, Tung, and Adamowicz carried out methodological developments to improve the convergence of the ECG wave function and energy, and to reduce the computational cost for polyatomic, *i.e.*, H₃⁺ and H₃, systems. Their efforts resulted in the most precise non-relativistic energy for H₃, so far, near the equilibrium structure [20].

The aim of the present letter is to explore and take the achievable precision further for H₃, a simple prototype for poly-electronic and poly-atomic molecular systems, using explicitly correlated Gaussian functions.

2. Method

The Schrödinger equation (in Hartree atomic units) with N_{nuc} nuclei clamped at the \mathbf{R} configuration and n_p electrons,

$$H\psi(\mathbf{r}; \mathbf{R}) = E(\mathbf{R})\psi(\mathbf{r}; \mathbf{R}) \quad (1)$$

*Corresponding author

Email address: edit.matyus@ttk.elte.hu (Edit Mátyus)

$$H = \frac{1}{2} \sum_{i=1}^{n_p} \mathbf{p}_i^2 - \sum_{a=1}^{N_{\text{nuc}}} \sum_{i=1}^{n_p} \frac{Z_a}{r_{ia}} + \sum_{i<j}^{n_p} \frac{1}{r_{ij}} + \sum_{a<b}^{N_{\text{nuc}}} \frac{Z_a Z_b}{R_{ab}}, \quad (2)$$

is solved for the ground state of H_3 using a set of floating ECG basis functions,

$$\psi(\mathbf{r}; \mathbf{R}) = \mathcal{A} \sum_{n=1}^{N_b} c_n \phi_n(\mathbf{r}; \mathbf{A}_n, \mathbf{s}_n) \chi_n(\vartheta) \quad (3)$$

$$\phi_n(\mathbf{r}; \mathbf{A}_n, \mathbf{s}_n) = \exp \left[-(\mathbf{r} - \mathbf{s}_n)^T \underline{\mathbf{A}}_n (\mathbf{r} - \mathbf{s}_n) \right], \quad (4)$$

where $\underline{\mathbf{A}}_n = \mathbf{A}_n \otimes I_3$, $\mathbf{A}_n \in \mathbb{R}^{n_p \times n_p}$ is the exponent matrix and $\mathbf{r}, \mathbf{s} \in \mathbb{R}^{3n_p}$ are the coordinate vectors of the electrons and the Gaussian centers, respectively. \mathcal{A} is the anti-symmetrization operator, and \mathbf{A} is parameterized in the $\mathbf{A} = \mathbf{L}^T \mathbf{L}$ Cholesky-form, with an \mathbf{L} lower-triangular matrix, to ensure positive definiteness of \mathbf{A} and square integrability of the basis functions. The A_1 symmetry (in the $C_{\infty v}$ point group) of the ground-state wave function is realized by constraining the Gaussian centers to the z axis.

The $\chi_n(\vartheta)$ three-particle spin function corresponding to the doublet multiplicity of the ground-state is obtained as a linear combination of the two possible couplings of the elementary, one-electron spin functions $\sigma(i)_{\frac{1}{2}, \pm \frac{1}{2}}$ to a doublet state [21],

$$\begin{aligned} \chi_n = & d_{n_1} \left[\left[\sigma(1)_{\frac{1}{2}} \sigma(2)_{\frac{1}{2}} \right]_{1,0} \sigma(3)_{\frac{1}{2}} \right]_{\frac{1}{2}, \frac{1}{2}} \\ & + d_{n_2} \left[\left[\sigma(1)_{\frac{1}{2}} \sigma(2)_{\frac{1}{2}} \right]_{0,0} \sigma(3)_{\frac{1}{2}} \right]_{\frac{1}{2}, \frac{1}{2}}, \quad (5) \end{aligned}$$

where the square brackets denote angular momentum coupling, using the Clebsch–Gordan coefficients $\langle j_1, m_{j_1}, j_2, m_{j_2} | J, M_J \rangle$. For example, coupling two spin-1/2 particles to a singlet function is labelled as

$$\begin{aligned} & \left[\sigma(1)_{\frac{1}{2}} \sigma(2)_{\frac{1}{2}} \right]_{0,0} \\ & = \left\langle \frac{1}{2}, \frac{1}{2}, \frac{1}{2}, -\frac{1}{2} \left| 0, 0 \right. \right\rangle \sigma(1)_{\frac{1}{2}, \frac{1}{2}} \sigma(2)_{\frac{1}{2}, -\frac{1}{2}} \\ & + \left\langle \frac{1}{2}, -\frac{1}{2}, \frac{1}{2}, \frac{1}{2} \left| 0, 0 \right. \right\rangle \sigma(1)_{\frac{1}{2}, -\frac{1}{2}} \sigma(2)_{\frac{1}{2}, \frac{1}{2}} \\ & = \frac{1}{\sqrt{2}} (|\uparrow\downarrow\rangle - |\downarrow\uparrow\rangle). \quad (6) \end{aligned}$$

Considering the normalization condition as well, the doublet three-electron spin functions can be parameterized by a single ϑ_n parameter as

$$d_{n_1} = \sin \vartheta_n \quad \text{and} \quad d_{n_2} = \cos \vartheta_n, \quad (7)$$

and ϑ_n is optimized together with the nonlinear parameters of the basis set.

2.1. Optimized fragment initialization

The initial basis function parameters are usually generated in a pseudo-random manner, retaining those functions from a trial set that provide the lowest energy expectation value. This generation procedure is followed by extensive refinement of the parameterization based on the variational principle [21]. By increasing the number of electrons, the dimensionality of the parameter space, and hence, the optimization cost increases. To keep the computational cost low, it is useful to consider that the interaction between the electrons of the hydrogen molecule and the electron of the hydrogen atom is weak in the van-der-Waals well or if the two ‘fragments’ are not too close, in general. If the interaction is not too strong, then a ψ_1 initial approximation for the wave function can be written as the product of the wave functions optimized for the ‘fragments’ (atom and molecule for the present example):

$$\begin{aligned} \psi_1^{\text{H}_3}(\mathbf{r}_1, \mathbf{r}_2, \mathbf{r}_3) & = \psi^{\text{H}_2}(\mathbf{r}_1, \mathbf{r}_2) \psi^{\text{H}}(\mathbf{r}_3) \\ & = \sum_{k,l} c_k c_l \phi_k^{\text{H}_2}(\mathbf{r}_1, \mathbf{r}_2) \phi_l^{\text{H}}(\mathbf{r}_3), \quad (8) \end{aligned}$$

which corresponds to an initial parameterization of the three-electron basis set with

$$\mathbf{A}_{kl}^{\text{I}} = \begin{pmatrix} \mathbf{A}_k^{\text{H}_2} & 0 \\ 0 & A_l^{\text{H}} \end{pmatrix}, \quad (9)$$

and the 3-electron \mathbf{s} vectors include the \mathbf{s} vectors shifted according to the configuration of the ‘fragments’ in H_3 :

$$\mathbf{s}_{kl}^{\text{I}} = \begin{pmatrix} \mathbf{s}_k^{\text{H}_2} + \mathbf{R}_{\text{CM}}^{\text{H}_2} \\ \mathbf{s}_l^{\text{H}} + \mathbf{R}^{\text{H}} \end{pmatrix}, \quad (10)$$

where $\mathbf{R}_{\text{CM}}^{\text{H}_2}$ is the center of mass of the protons in H_2 .

This procedure is reminiscent of the monomer contraction method that was first introduced in Ref. [22] for the helium dimer, although there are a few differences. First, we use the fragment (or monomer) basis set only to initialize the many(three)-electron basis, and we run repeated refinement cycles [23, 24] using the Powell method [25] for this initial basis. Second, retaining the full direct-product basis optimized for H_2 and separately for H would be computationally very demanding, so instead, we truncate the direct-product basis according to the following strategy.

The ground-state wave function of the H_2 molecule was expanded over 1200 ECG functions, yielding $-1.174\,475\,714\,E_h$ for the ground state energy, which—compared to the

most accurate value obtained by Pachucki $-1.174\,475\,714\,220\,4434(5) E_h$ [26]—is converged to a fraction of a nE_h . The wave function of the hydrogen atom was represented with 10 optimized Gaussian functions, resulting in $-0.499\,999\,332 E_h$ (in comparison with the exact value, $-0.5 E_h$) ground-state energy. Inclusion of all possible combinations of the H_2 and H basis functions would result in a gigantic, 12 000-term expansion. Such a long expansion would be prohibitively expensive to extensively optimize (refine), and it is unnecessary to have so many functions for the reaching a $1 : 10^9$ (ppb) precision. To reduce the direct-product basis, it would be possible to perform competitive selection over the large basis space or to order (and then truncate) the basis functions based on their importance in lowering the energy [21]. In the present work, we used a very simple construct that does not require any computation: we have generated a set of 1200 functions by appending each H_2 basis function from the 1200 set with a single H function. Out of the 10 H functions, we have picked one based on the basis index, *i.e.*,

$$\begin{aligned} & \{ \phi_{10n+i}^{H_2} \phi_i^H; n = 0, 1, \dots, 119, i = 1, 2, \dots, 10 \} \\ & = \{ \phi_1^{H_2} \phi_1^H, \phi_2^{H_2} \phi_2^H, \dots, \phi_{10}^{H_2} \phi_{10}^H, \\ & \quad \phi_{11}^{H_2} \phi_1^H, \phi_{12}^{H_2} \phi_2^H, \dots, \phi_{20}^{H_2} \phi_{10}^H, \\ & \quad \dots \\ & \quad \phi_{1191}^{H_2} \phi_1^H, \phi_{1192}^{H_2} \phi_2^H, \dots, \phi_{1200}^{H_2} \phi_{10}^H \} . \end{aligned} \quad (11)$$

The spin basis functions defined in Eq. (5), were initialized by coupling the two electrons initially localized on the H_2 fragment to a singlet state, *i.e.*, $d_{n_1} = 0$ and $d_{n_2} = 1$ corresponding to $\vartheta_n = 0$ ($n = 1, 2, \dots, 1200$) in Eqs. (5)–(7). All non-linear parameters, including ϑ_n , of the initial basis set were excessively optimized in repeated refinement cycles (Fig. 1). The optimized fragment-based initialization of the basis set, described in this section, allowed saving several weeks (months) of computer time in comparison with Ref. [27] (see also Sec. 3).

2.2. Gaussian-center scaling

Independent variational optimization of the basis set at many points along the PEC (or over the PES) would make the computations very computationally intensive. Kołos and Wolniewicz [28] noted already in 1964 that for a sufficiently large basis set, the A_k exponents are insensitive to small displacements of the nuclear coordinates. In 1997, Cencek and Kutzelnigg proposed a scaling technique to generate a good initial ECG (re)parameterization for the electronic basis set of diatomics upon small nu-

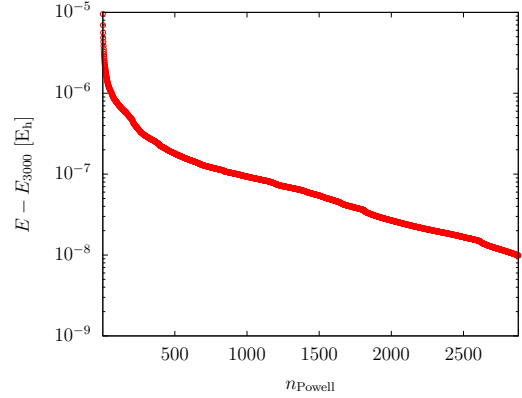


Figure 1: Convergence of the ground-state energy of $H_2 \cdots H$ during the course of the Powell refinement cycles (n_{Powell}) of $N_b = 1200$ basis functions initialized using basis functions optimized for the fragments, Eq. (11). $R_{H_2} = 1.4$ bohr and $R_{H_2 \cdots H} = 6.442$ bohr, $E_{3000} = -1.674\,561\,687 E_h$. (See also Table 1.)

clear displacements [29]. They noted that their approach can be generalized beyond diatomics. Pavanello and Adamowicz implemented rescaling the ECG centers (to have a good starting basis set) of H_3^+ upon small nuclear displacements to generate a series of points to represent the 3D PES [27, 30, 31, 32]. Upon a small $\Delta \mathbf{R}_a$ displacement of the coordinates of the a th nucleus,

$$\mathbf{R}'_a = \mathbf{R}_a + \Delta \mathbf{R}_a , \quad (12)$$

the $\mathbf{s}_i \in \mathbb{R}^3$ ECG centers corresponding to the i th electron were transformed as

$$\mathbf{s}'_i = \mathbf{s}_i + \Delta \mathbf{s}_i , \quad (13)$$

where $\Delta \mathbf{s}_i$ is expressed as a function of the $\Delta \mathbf{R}_a$ nuclear displacement,

$$\Delta \mathbf{s}_i = \frac{1}{W_i} \sum_{a=1}^{N_{\text{nuc}}} w_{ia} \Delta \mathbf{R}_a \quad (14)$$

with $W_i = \sum_{a=1}^{N_{\text{nuc}}} w_{ia}$. The w_{ia} ‘weight’ is a function constructed based on simple arguments. It is chosen to be the distance of the \mathbf{s}_i center and the a th nucleus, $|\mathbf{s}_i - \mathbf{R}_a|$ and it is expected to have good limiting properties. First, it must vanish if the \mathbf{s}_i center is very (infinitely) far from the displaced nucleus, $\lim_{|\mathbf{s}_i - \mathbf{R}_a| \rightarrow \infty} w_{ia} = 0$. Second, the closer the \mathbf{s}_i center to the \mathbf{R}_a nucleus position, the $\Delta \mathbf{R}_a$ displacement has a larger contribution, *i.e.*, larger w_{ia} weight, to the $\Delta \mathbf{s}_i$ change.

These conditions allow several possible choices for the weight function. For example, Coulomb-

like weights were used in Ref. [27]

$$w_{ia}^C = \frac{1}{|s_i - \mathbf{R}_a|}. \quad (15)$$

After some experimentation with different possible functions, and inspired by the picture that the weight function can be intuitively defined as if there was some attraction between the centers and the nuclear positions by a central field, a Yukawa-like weight function appears to be a good choice

$$w_{ia}^Y = \frac{e^{-\mu|s_i - \mathbf{R}_a|}}{|s_i - \mathbf{R}_a|}, \quad (16)$$

where the parameter $\mu \in \mathbb{R}^+$ was set to unity in this work. For small nuclear displacements, a parameterization rescaled with Yukawa weights (with $\mu = 1$) provided an energy lower than rescaling with Coulomb weights, Eq. (15).

The rescaling technique with the Yukawa weight function was used to generate the PEC corresponding to the H atom approaching the H₂ molecule with a proton-proton distance fixed at $R_{\text{H}_2} = 1.4$ bohr. The $R_{\text{H}_2 \dots \text{H}}$ distance of the hydrogen atom was measured from the center of mass of the H₂ fragment. The starting value was $R_{\text{H}_2 \dots \text{H}} = 6.442$ bohr, for which an initial basis set was generated using the optimized fragment initialization (Sec. 2.1) and the representation was improved through several Powell refinement [25] cycles of the non-linear parameters (Fig. 1). Then, initial basis sets were generated by making small $\Delta R_{\text{H}_2 \dots \text{H}} = \pm 0.1$ bohr displacements, rescaling the centers according to Eq. (14) with Yukawa weights, Eq. (16), followed by 5 entire basis refinement cycles (that took 4 hours) before the next step was taken along the series of the nuclear configurations (the positive and the negative displacement series were run in parallel). All computations have been carried out using the QUANTEN computer program [24, 33, 34, 35].

The energies (Fig. 2) and optimized basis set parameters are deposited in the Supplementary Material.

3. Results and discussion

We have carried out extensive single-point computations for the near-equilibrium geometry in the van-der-Waals well with $R_{\text{H}_2}^{(0)} = 1.4$ bohr and $R_{\text{H}_2 \dots \text{H}}^{(0)} = 6.442$ bohr first reported in Ref. [19]. This structure is close to the equilibrium geometry obtained with carefully conducted orbital-based computations [17] (Table 2). The energy of Ref. [19] computed with a small ECG basis is inaccurate, but later, large-scale computations were reported in Ref. [20].

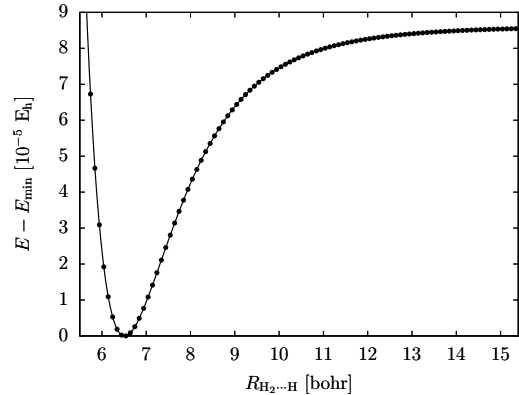


Figure 2: Potential energy cut of the H₃ system converged in the present work with an estimated sub-ppm precision. Along the curve, the geometry of the H₂ unit is fixed at $R_{\text{H}_2} = 1.4$ bohr. The lowest-energy datapoint corresponds to $E_{\text{min}} = -1.674\,561\,899\,E_h$ and $R_{\text{min}} = 6.542$ bohr.

At this geometry, the best energy obtained from the present work with 1200 ECGs (constructed by the initial fragment initialization, Sec. 2.1, followed by $n_{\text{Powell}} = 3000$ Powell refinement cycles of the entire basis set) is $-1.674\,561\,687\,E_h$ (upper part of Table 1). Table 1 also shows the computed energy values for smaller basis sets that allow assessment of the convergence and extrapolation to the complete basis set (CBS) limit [36].

Direct comparison with Ref. [20] requires further computation, because the extensively optimized energy reported in Ref. [20] appears to belong to a 6.442 bohr distance of the hydrogen atom not from the center of nuclear mass of the H₂ unit, but from the closer proton of H₂. We think that this nuclear structure was used in Ref. [20], because we obtain good agreement for the energies when we perform the computation at this geometry, shown in the lower part of Table 1, corresponding to $R_{\text{H}_2}^{(0)} = 1.40$ bohr and $R_{\text{H}_2 \dots \text{H}}' = R_{\text{H}_2 \dots \text{H}}^{(0)} + R_{\text{H}_2}^{(0)}/2 = 6.442$ bohr + 0.700 bohr = 7.142 bohr.

We also note that the best energy value of Ref. [20] computed in 6 months (using 12 CPU cores) was reproduced in this work (corresponding to the structure given in footnote ^b of Table 1) using the optimized fragment initialization technique (Sec. 2.1) followed by a few Powell refinement cycles in 4 days. The computational benefit of the optimized fragment technique is significant in comparison with a computation [20] constructed from ‘scratch’ immediately for the three-particle problem.

Then, we continued the extensive refinement of the basis parameterization based on the variational

Table 1: Convergence of the non-relativistic, ground-state energy of H_3 near the van-der-Waals equilibrium structure at $R_{H_2} = 1.4$ bohr and $R_{H_2\dots H} = 6.442$ bohr taken from Ref. [19].

N_b	Ansatz	n_{Powell}	E [E_h]
$R_{H_2} = 1.40$ bohr, $R_{H_2\dots H} = 6.442$ bohr: ^a			
600	$\{\psi_{10n+i}^{H_2} \cdot \psi_i^H\}$	2000	-1.674 560 470
800	$\{\psi_{10n+i}^{H_2} \cdot \psi_i^H\}$	2000	-1.674 561 379
1000	$\{\psi_{10n+i}^{H_2} \cdot \psi_i^H\}$	2000	-1.674 561 583
1200	$\{\psi_{10n+i}^{H_2} \cdot \psi_i^H\}$	3000	-1.674 561 687
[Extrapolation to $N_b \rightarrow \infty$:			-1.674 561 75(3)]
$R_{H_2} = 1.40$ bohr, $R_{H_2\dots H} = 7.142$ bohr: ^b			
1000	Ref. [20] ^c		-1.674 547 421 00
1200	$\{\psi_{10n+i}^{H_2} \cdot \psi_i^H\}$	3000	-1.674 547 750

^a $R_{H_2} = 1.4$ bohr, $R_{H_2\dots H} = 6.442$ bohr, measured from the nuclear center of mass (NCM) of the H_2 unit.

^b $R_{H_2} = 1.4$ bohr, $R_{H_2\dots H} = 7.142$ bohr (measured from the NCM of the H_2 unit), and corresponds to a 6.442 bohr distance measured from the nearer proton in the H_2 unit.

^c Geometry ^a is claimed in Ref. [20], but it appears to be ^b. The difference amounts to whether the distance of the hydrogen atom is measured from the NCM or the nearer proton.

principle, and the best result after 3 months computation (using 12 CPU cores) is reported in Table 1. The generation of the points along the PEC was started from this well-optimized parameterization by $\Delta R_{H_2\dots H} = \pm 0.1$ bohr increments/decrements (running in parallel) using the rescaling technique (Sec. 2.1), followed by 5 Powell refinement cycles at every step (before the next step was taken). The entire PEC generation took took 13 days using 12 CPU cores.

Finally, it is relevant to compare the ECG energies with the best orbital-based results underlying the CCI PES. For this reason, we have used a single rescaling step from the starting optimized parameterization (upper part of Table 1) to the $R_{H_2}^{(0)} = 1.4$ bohr and $R_{H_2\dots H}^{(0)} = 6.51205$ bohr structure, which was determined to be the global minimum structure at the MRCI/aug-cc-pV6Z level [17]. The parameter rescaling, with a negligible computational cost, was followed by 5 Powell refinement cycles that took 4 hours. Table 2 shows the energy values reported for the MRCI computations corresponding to the aug-cc-pVXZ ($X = D, T, Q, 5, 6$) and the ‘modified’ correlation consistent aug-mcc-pVXZ ($X = D, T, Q, 5, 6, 7$) basis sets [17, 14]. The ECG energy is already $74 \mu E_h$ lower, than the best MRCI value corresponding to the largest (aug-

mcc-pV7Z) basis set. Furthermore, we can confirm the estimated μE_h precision of the CBS extrapolated energy from the mcc basis, whereas the extrapolated energy based on the regular correlation consistent basis is slightly lower than our current best estimate [17].

Table 2: Comparison of energies of various *ab initio* computations. The equilibrium geometry, determined at the MRCI/aug-cc-pV6Z is $R_{H_2} = 1.4015$ bohr and $R_{H_2\dots H} = 6.51205$ bohr [17].

Source	E [E_h]
aug-cc-pVDZ ^a	-1.664 339
aug-cc-pVTZ ^a	-1.672 540
aug-cc-pVQZ ^a	-1.673 902
aug-cc-pV5Z ^a	-1.674 332
aug-cc-pV6Z ^a	-1.674 445
aug-mcc-pVTZ ^a	-1.672 553
aug-mcc-pVQZ ^a	-1.673 917
aug-mcc-pV5Z ^a	-1.674 298
aug-mcc-pV6Z ^a	-1.674 430
aug-mcc-pV7Z ^a	-1.674 488
MBE ^{cc} (3,4 CBS) ^b	-1.674 566
MBE ^{mcc} (6,7 CBS) ^c	-1.674 562
Present work ($N_b = 1200$) ^d	-1.674 562 264

^a Ref. [17]: MRCI energy.

^{b, c} Ref. [17]: extrapolated CBS energy

corresponding to the aug-cc-pVXZ ($X = 3, 4$) and aug-mcc-pVXZ ($X = 6, 7$) basis sets, respectively.

^d Rescaled from the basis set optimized for the ($R_{H_2}^{(0)}, R_{H_2\dots H}^{(0)}$) structure in Table 1 followed by 1000 Powell refinement cycles.

4. Summary, conclusion, and outlook

In summary, we have computed a benchmark-quality one-dimensional segment of the Born–Oppenheimer potential energy surface of the H_3 system for a series of collinear nuclear configurations. The electronic energies are estimated to be converged on the sub-parts-per-million level.

The depth of the van-der-Waals well was predicted to be $86(1) \mu E_h$ at the $R_{H_2} = 1.4015$ bohr and $R_{H_2\dots H} = 6.51205$ bohr geometry in MRCI computations underlying the currently most precise potential energy surface of H_3 [17]. The variational computations reported in this work and using a (relatively small) explicitly correlated Gaussian basis set confirm this value and improve upon its precision by two orders of magnitude, $86.54(3) \mu E_h$. In order to achieve a similar precision for non-collinear nuclear structures, which have a lower order or no point-group symmetry, it will be necessary to use a larger basis set, which is certainly feasible.

Regarding the broader context of this work, (non-)adiabatic perturbation theory [37, 38, 39, 40, 41] combined with leading-order relativistic and quantum electrodynamics (QED) corrections [42, 43] are expected to provide a state-of-the-art theoretical description for this system. This framework has already been extensively used and tested for the lightest diatomic molecules [44, 35]. For the ground-electronic state of the H_2 molecule, the effect of the non-adiabatic-relativistic coupling has also been evaluated and was found to be non-negligible [45]. In this direction, the computation of a precise representation of the electronic wave function is a necessary first step that was demonstrated in this work to be feasible. The adiabatic, non-adiabatic and (regularized) relativistic and QED corrections can be evaluated at a couple of points using currently existing procedures [41, 46, 35, 47]. At the same time, for a complete description of a polyatomic system like H_3 , these corrections must be computed over hundreds or thousands of nuclear configurations. This requires a fully automated evaluation and error control of all corrections, which may be especially challenging for the singular terms in the relativistic and QED expressions, and this requires further methodological and algorithmic developments that is left for future work.

5. Acknowledgment

Financial support of the European Research Council through a Starting Grant (No. 851421) is gratefully acknowledged. DF thanks a doctoral scholarship from the ÚNKP-21-3 New National Excellence Program of the Ministry for Innovation and Technology from the source of the National Research, Development and Innovation Fund (ÚNKP-21-3-II-ELTE-41). We also thank Péter Jeszenszki for discussions about energy extrapolation for ECG basis sets.

References

- [1] F. J. Aoiz, L. B. Nares, V. J. Herrero, The $H+H_2$ reactive system. Progress in the study of the dynamics of the simplest reaction, *Int. Rev. Phys. Chem.* 24 (1) (2005) 119–190. doi:10.1080/01442350500195659.
- [2] B. Liu, Ab initio potential energy surface for linear H_3 , *J. Chem. Phys.* 58 (5) (1973) 1925–1937. doi:10.1063/1.1679454.
- [3] P. Siegbahn, B. Liu, An accurate three-dimensional potential energy surface for H_3 , *J. Chem. Phys.* 68 (5) (1978) 2457–2465. doi:10.1063/1.436018.
- [4] D. G. Truhlar, C. J. Horowitz, Functional representation of Liu and Siegbahn’s accurate ab initio potential energy calculations for $H+H_2$, *J. Chem. Phys.* 68 (5) (1978) 2466–2476. doi:10.1063/1.436019.
- [5] A. J. C. Varandas, F. B. Brown, C. A. Mead, D. G. Truhlar, N. C. Blais, A double many-body expansion of the two lowest-energy potential surfaces and nonadiabatic coupling for H_3 , *J. Chem. Phys.* 86 (11) (1987) 6258–6269. doi:10.1063/1.452463.
- [6] A. I. Boothroyd, W. J. Keogh, P. G. Martin, M. R. Peterson, An improved H_3 potential energy surface, *J. Chem. Phys.* 95 (6) (1991) 4343–4359. doi:10.1063/1.461758.
- [7] A. I. Boothroyd, W. J. Keogh, P. G. Martin, M. R. Peterson, A refined H_3 potential energy surface, *J. Chem. Phys.* 104 (18) (1996) 7139–7152. doi:10.1063/1.471430.
- [8] Y.-S. Wu, J. Anderson, et al., A very high accuracy potential energy surface for H_3 , *Phys. Chem. Chem. Phys.* 1 (6) (1999) 929–937. doi:10.1039/A808797K.
- [9] D. L. Diedrich, J. B. Anderson, Exact quantum Monte Carlo calculations of the potential energy surface for the reaction $H+H_2 \rightarrow H_2+H$, *J. Chem. Phys.* 100 (11) (1994) 8089–8095. doi:10.1063/1.466802.
- [10] M. R. A. Blomberg, B. Liu, The H_3 potential surface revisited, *J. Chem. Phys.* 82 (2) (1985) 1050–1051. doi:10.1063/1.448527.
- [11] C. W. Bauschlicher, S. R. Langhoff, H. Partridge, A reevaluation of the H_3 potential, *Chem. Phys. Lett.* 170 (4) (1990) 345–348. doi:10.1016/S0009-2614(90)87029-Q.
- [12] H. Partridge, C. W. Bauschlicher, J. R. Stallcop, E. Levin, Ab initio potential energy surface for $H-H_2$, *J. Chem. Phys.* 99 (8) (1993) 5951–5960. arXiv:10.1063/1.465894, doi:10.1063/1.465894.
- [13] D. L. Diedrich, J. B. Anderson, An accurate quantum Monte Carlo calculation of the barrier height for the reaction $H+H_2 \rightarrow H_2+H$, *Science* 258 (5083) (1992) 786–788. doi:10.1126/science.258.5083.786.
- [14] S. L. Mielke, B. C. Garrett, K. A. Peterson, The utility of many-body decompositions for the accurate basis set extrapolation of ab initio data, *J. Chem. Phys.* 111 (9) (1999) 3806–3811. doi:10.1063/1.479683.
- [15] K. E. Riley, J. B. Anderson, Higher accuracy quantum Monte Carlo calculations of the barrier for the $H+H_2$ reaction, *J. Chem. Phys.* 118 (7) (2003) 3437–3438. doi:10.1063/1.1527012.
- [16] H.-X. Huang, Exact Fixed-node Quantum Monte Carlo: Differential Approach, *Chin. J. Chem. Phys.* 23 (11) (2005) 1474–1478. doi:10.1002/cjoc.200591474.
- [17] S. L. Mielke, B. C. Garrett, K. A. Peterson, A hierarchical family of global analytic Born–Oppenheimer potential energy surfaces for the $H+H_2$ reaction ranging in quality from double-zeta to the complete basis set limit, *J. Chem. Phys.* 116 (10) (2002) 4142–4161. doi:10.1063/1.1432319.
- [18] S. L. Mielke, K. A. Peterson, D. W. Schwenke, B. C. Garrett, D. G. Truhlar, J. V. Michael, M.-C. Su, J. W. Sutherland, $H+H_2$ Thermal Reaction: A Convergence of Theory and Experiment, *Phys. Rev. Lett.* 91 (2003) 063201. doi:10.1103/PhysRevLett.91.063201.
- [19] M. Cafiero, L. Adamowicz, Simultaneous optimization of molecular geometry and the wave function in a basis of Singer’s n -electron explicitly correlated Gaussians, *Chem. Phys. Lett.* 335 (5) (2001) 404–408. doi:10.1016/S0009-2614(01)00086-0.
- [20] M. Pavanello, W.-C. Tung, L. Adamowicz, How to calculate H_3 better, *J. Chem. Phys.* 131 (18) (2009) 184106. doi:10.1063/1.3257592.
- [21] Y. Suzuki, K. Varga, Stochastic Variational Approach to Quantum-Mechanical Few-Body Problems, Springer-Verlag, Berlin, Heidelberg, 1998.
- [22] W. Cencek, J. Komasa, K. Pachucki, K. Szalewicz, Relativistic Correction to the Helium Dimer Interaction Energy, *Phys. Rev. Lett.* 95 (2005) 233004. doi:10.1103/PhysRevLett.95.233004.

- [23] E. Mátyus, M. Reiher, Molecular structure calculations: a unified quantum mechanical description of electrons and nuclei using explicitly correlated Gaussian functions and the global vector representation, *J. Chem. Phys.* 137 (2012) 024104. doi:10.1063/1.4731696.
- [24] E. Mátyus, Pre-Born–Oppenheimer molecular structure theory, *Mol. Phys.* 117 (5) (2019) 590–609. doi:10.1080/00268976.2018.1530461.
- [25] M. J. D. Powell, The NEWUOA software for unconstrained optimization without derivatives (DAMTP 2004/NA05), Report no. NA2004/08, <http://www.damtp.cam.ac.uk/user/na/reports04.html> last accessed on January 18, 2013.
- [26] K. Pachucki, Born–Oppenheimer potential for H₂, *Phys. Rev. A* 82 (2010) 032509. doi:10.1103/PhysRevA.82.032509.
- [27] M. Pavanello, L. Adamowicz, High-accuracy calculations of the ground, 1 ¹A₁⁺, and the 2 ¹A₁⁺, 2 ³A₁⁺, and 1 ¹E' excited states of H₃⁺, *J. Chem. Phys.* 130 (3) (2009) 034104. doi:10.1063/1.3058634.
- [28] W. Kołos, L. Wolniewicz, Accurate Adiabatic Treatment of the Ground State of the Hydrogen Molecule, *J. Chem. Phys.* 41 (12) (1964) 3663–3673. doi:10.1063/1.1725796.
- [29] W. Cencek, W. Kutzelnigg, Accurate adiabatic correction for the hydrogen molecule using the Born–Handy formula, *Chem. Phys. Lett.* 266 (3-4) (1997) 383–387. doi:10.1016/S0009-2614(97)00017-1.
- [30] M. Pavanello, W.-C. Tung, F. Leonarski, L. Adamowicz, New more accurate calculations of the ground state potential energy surface of H₃⁺, *J. Chem. Phys.* 130 (7) (2009) 074105. doi:10.1063/1.3077193.
- [31] L. Adamowicz, M. Pavanello, Progress in calculating the potential energy surface of H₃⁺, *Philos. Trans. R. Soc. A* 370 (1978) (2012) 5001–5013. doi:10.1098/rsta.2012.0101.
- [32] M. Pavanello, L. Adamowicz, A. Alijah, N. F. Zobov, I. I. Mizus, O. L. Polyansky, J. Tennyson, T. Szidarovszky, A. G. Császár, Calibration-quality adiabatic potential energy surfaces for H₃⁺ and its isotopologues, *J. Chem. Phys.* 136 (18) (2012) 184303. doi:10.1063/1.4711756.
- [33] D. Ferenc, E. Mátyus, Non-adiabatic mass correction for excited states of molecular hydrogen: Improvement for the outer-well $HH^+ \ ^1\Sigma_g^+$ term values, *J. Chem. Phys.* 151 (9) (2019) 094101, publisher: American Institute of Physics. doi:10.1063/1.5109964.
- [34] D. Ferenc, E. Mátyus, Computation of rovibronic resonances of molecular hydrogen: $EF \ ^1\Sigma_g^+$ inner-well rotational states, *Phys. Rev. A* 100 (2) (2019) 020501. doi:10.1103/PhysRevA.100.020501.
- [35] D. Ferenc, V. I. Korobov, E. Mátyus, Nonadiabatic, Relativistic, and Leading-Order QED Corrections for Rovibrational Intervals of ⁴He₂⁺ ($X^2\Sigma_u^+$), *Phys. Rev. Lett.* 125 (2020) 213001. doi:10.1103/PhysRevLett.125.213001.
- [36] P. Kopta, T. Piontek, K. Kurowski, M. Puchalski, J. Komasa, Convergence of Explicitly Correlated Gaussian Wave Functions, in: *EScience on Distributed Computing Infrastructure - Volume 8500*, Springer-Verlag, Berlin, Heidelberg, 2014, p. 459–474. doi:10.1007/978-3-319-10894-0_33.
- [37] S. Teufel, *Adiabatic perturbation theory in quantum dynamics*, Lecture Notes in Mathematics, Springer, 2003.
- [38] G. Panati, H. Spohn, S. Teufel, The time-dependent Born–Oppenheimer approximation, *ESAIM: Math. Mod. Num. Anal.* 41 (2007) 297. doi:10.1051/m2an:2007023.
- [39] K. Pachucki, J. Komasa, Nonadiabatic corrections to the wave function and energy, *J. Chem. Phys.* 129 (2008) 034102. doi:10.1063/1.2952517.
- [40] E. Mátyus, S. Teufel, Effective non-adiabatic Hamiltonians for the quantum nuclear motion over coupled electronic states, *J. Chem. Phys.* 151 (2019) 014113. doi:10.1063/1.5097899.
- [41] E. Mátyus, D. Ferenc, Vibronic mass computation for the $EF-GK-HH \ ^1\Sigma_g^+$ manifold of molecular hydrogen, *Mol. Phys.* (2022).
- [42] H. Araki, Quantum-electrodynamical corrections to energy-levels of helium, *Prog. of Theor. Phys.* 17 (1957) 619–642. doi:10.1143/PTP.17.619.
- [43] J. Sucher, Energy levels of the two-electron atom, to order α^3 Rydberg (Columbia University) (1958).
- [44] J. Komasa, M. Puchalski, P. Czachorowski, G. Łach, K. Pachucki, Rovibrational energy levels of the hydrogen molecule through nonadiabatic perturbation theory, *Phys. Rev. A* 100 (2019) 032519. doi:10.1103/PhysRevA.100.032519.
- [45] P. Czachorowski, M. Puchalski, J. Komasa, K. Pachucki, Nonadiabatic relativistic correction in H₂, D₂, and HD, *Phys. Rev. A* 98 (2018) 052506. doi:10.1103/PhysRevA.98.052506.
- [46] K. Pachucki, W. Cencek, J. Komasa, On the acceleration of the convergence of singular operators in Gaussian basis sets, *J. Chem. Phys.* 122 (18) (2005) 184101. doi:10.1063/1.1888572.
- [47] P. Jeszenszki, R. T. Ireland, D. Ferenc, E. Mátyus, On the inclusion of cusp effects in expectation values with explicitly correlated Gaussians, *Int. J. Quant. Chem.* (2021). doi:doi.org/10.1002/qua.26819.

Supplementary Material

Table 3: Potential energy curve of collinear H₃, with collinear hydrogen atoms and the H₂ structure fixed at $R_{H_2} = 1.4$ bohr.

$R_{H_2 \dots H}$ [bohr]	E [E _h]	$R_{H_2 \dots H}$ [bohr]	E [E _h]	$R_{H_2 \dots H}$ [bohr]	E [E _h]
3.942	-1.671 027 070	7.742	-1.674 527 262	11.542	-1.674 480 330
4.042	-1.671 542 481	7.842	-1.674 524 133	11.642	-1.674 480 079
4.142	-1.671 995 736	7.942	-1.674 521 142	11.742	-1.674 479 843
4.242	-1.672 392 125	8.042	-1.674 518 294	11.842	-1.674 479 622
4.342	-1.672 736 967	8.142	-1.674 515 593	11.942	-1.674 479 415
4.442	-1.673 035 388	8.242	-1.674 513 039	12.042	-1.674 479 220
4.542	-1.673 292 312	8.342	-1.674 510 633	12.142	-1.674 479 036
4.642	-1.673 512 388	8.442	-1.674 508 369	12.242	-1.674 478 864
4.742	-1.673 699 926	8.542	-1.674 506 245	12.342	-1.674 478 702
4.842	-1.673 858 896	8.642	-1.674 504 254	12.442	-1.674 478 549
4.942	-1.673 992 934	8.742	-1.674 502 391	12.542	-1.674 478 405
5.042	-1.674 105 325	8.842	-1.674 500 651	12.642	-1.674 478 269
5.142	-1.674 198 999	8.942	-1.674 499 026	12.742	-1.674 478 141
5.242	-1.674 276 566	9.042	-1.674 497 510	12.842	-1.674 478 020
5.342	-1.674 340 341	9.142	-1.674 496 096	12.942	-1.674 477 906
5.442	-1.674 392 365	9.242	-1.674 494 779	13.042	-1.674 477 799
5.542	-1.674 434 419	9.342	-1.674 493 552	13.142	-1.674 477 697
5.642	-1.674 468 056	9.442	-1.674 492 409	13.242	-1.674 477 601
5.742	-1.674 494 619	9.542	-1.674 491 345	13.342	-1.674 477 510
5.842	-1.674 515 270	9.642	-1.674 490 355	13.442	-1.674 477 424
5.942	-1.674 531 005	9.742	-1.674 489 433	13.542	-1.674 477 343
6.042	-1.674 542 675	9.842	-1.674 488 574	13.642	-1.674 477 266
6.142	-1.674 551 007	9.942	-1.674 487 775	13.742	-1.674 477 193
6.242	-1.674 556 616	10.042	-1.674 487 030	13.842	-1.674 477 124
6.342	-1.674 560 021	10.142	-1.674 486 337	13.942	-1.674 477 058
6.442	-1.674 561 676	10.242	-1.674 485 691	14.042	-1.674 476 996
6.542	-1.674 561 899	10.342	-1.674 485 088	14.142	-1.674 476 937
6.642	-1.674 561 042	10.442	-1.674 484 527	14.242	-1.674 476 880
6.742	-1.674 559 343	10.542	-1.674 484 003	14.342	-1.674 476 827
6.842	-1.674 557 010	10.642	-1.674 483 515	14.442	-1.674 476 777
6.942	-1.674 554 214	10.742	-1.674 483 058	14.542	-1.674 476 728
7.042	-1.674 551 095	10.842	-1.674 482 632	14.642	-1.674 476 683
7.142	-1.674 547 764	10.942	-1.674 482 234	14.742	-1.674 476 639
7.242	-1.674 544 313	11.042	-1.674 481 862	14.842	-1.674 476 598
7.342	-1.674 540 812	11.142	-1.674 481 514	14.942	-1.674 476 559
7.442	-1.674 537 318	11.242	-1.674 481 188	15.042	-1.674 476 521
7.542	-1.674 533 875	11.342	-1.674 480 883	15.142	-1.674 476 485
7.642	-1.674 530 514	11.442	-1.674 480 598	15.242	-1.674 476 451